Multidimensional two-photon imaging and spectroscopy of fresh human bladder biopsies

Riccardo Cicchi*[,a], Alfonso Crisci[b], Alessandro Cosci[a], Gabriella Nesi[c], Saverio Giancane[c], Marco Carini[c], and Francesco S. Pavone[a]

[a]European Laboratory for Non-linear Spectroscopy (LENS) and Department of Physics, University of Florence, 1 Via Nello Carrara, 50019 Sesto Fiorentino, Italy

[b]University of Florence Medical School, Department of Surgical and Medical Critical Area, University of Florence, Florence, Italy

[c]Division of Urology, Department of Surgical and Medical Critical Area, University of Florence, Florence, Italy

ABSTRACT

Two-photon microscopy has been successfully used to image several types of tissues, including skin, muscles, tendons. Nevertheless, its usefulness in imaging bladder tissue has not been investigated yet. In this work we used combined two-photon excited fluorescence, second-harmonic generation microscopy, fluorescence lifetime imaging microscopy, and multispectral two-photon emission detection to investigate different kinds of human *ex-vivo* fresh biopsies of bladder. Morphological and spectroscopic analyses allowed to characterize both healthy mucosa and carcinoma in-situ samples in a good agreement with common routine histology. Cancer cells showed different morphology with respect to the corresponding healthy cells: they appeared more elongated and with a larger nucleus to cytoplasm ratio. From the spectroscopic point of view, differences between the two tissue types in both spectral emission and fluorescence lifetime distribution were found. Even if further analysis, as well as a more significant statistics on a larger number of samples would be helpful to discriminate between low, mild, and high grade cancer, our method is a promising tool to be used as diagnostic confirmation of histological results, as well to be implemented in a multi-photon endoscope or in a spectroscopic for in *in-vivo* imaging applications.

Keywords: Non-linear microscopy, Urology

1. INTRODUCTION

Bladder cancer is one of the most diffused cancer in U.S. [1] Even if it is curable when detected and treated early, a more accurate early diagnosis of bladder cancer would be a suitable aim for both detection and treatment. Diagnostic methods used are different, even if a non-invasive early detection of bladder cancer is still a challenge. Very often, symptomatic patients are visually inspected through white light cystoscopy, which is the most diffused endoscopic technique for bladder cancer detection. This technique is only able to visualize the urothelium surface, limiting its diagnostic performance. Both sensitivity and specificity of cystoscopy can be improved by means of fluorescence, especially when high contrast agents are used. [2-4] Photosensitizers as such methyl-aminolevulinate can be used to enhance cancer margins contrast. Recently, non-invasive techniques, using both optical and non-optical methods, have been used in bladder cancer detection.

Two-photon excited (TPEF) fluorescence microscopy is a high-resolution laser imaging technique enabling deep tissue imaging. [5,6] Since both cells and extracellular matrix intrinsically contain a variety of fluorescent molecules (NADH, tryptophan, keratins, melanin, elastin, cholecalciferol and others), biological tissues can be imaged by TPEF microscopy without any exogenously added probe. [7-9] Additional morphological information can be provided by second harmonic generation (SHG) microscopy, which can be combined with TPEF microscopy using the same laser source. SHG has already been largely used for imaging non-centrosymmetric molecules inside cells [10,11] and

*rcicchi@lens.unifi.it, phone: +39 055 4572476; fax: +39 055 4572451; web: www.lens.unifi.it/bio

Photonic Therapeutics and Diagnostics VI, edited by N. Kollias, B. Choi, H. Zeng, R. S. Malek, B. J.-F. Wong, J. F. R. Ilgner, K. W. Gregory, G. J. Tearney, L. Marcu, H. Hirschberg, S. J. Madsen, A. Mandelis, A. Mahadevan-Jansen, E. D. Jansen, Proc. of SPIE Vol. 7548, 75480V · © 2010 SPIE · CCC code: 1605-7422/10/$18 · doi: 10.1117/12.841694

tissues [12-14]. Collagen fibers produce a high second harmonic signal [13] and can be imaged inside skin dermis with SHG microscopy [9,15]. Fluorescence lifetime imaging microscopy (FLIM) is an additional non-invasive microscopy technique enabling the identification of endogenous fluorescence species and their surrounding medium by measuring the decay rate of fluorescent emission. [16,17] FLIM is useful to study protein localization [18] and fluorescent molecular environment. [19] Multispectral two-photon (MTPE) tissue imaging can also be performed by measuring the two-photon emission spectra of different tissue proteins. This technique offers functional information about the relative quantities of fluorescent molecules, which correlate with tissue structure in physiological and pathological states. [20]

In this work we performed a multidimensional analysis [21] on bladder fresh biopsies by using non-linear microscopy with combined techniques (TPEF, FLIM, MTPE), all enabling deep imaging inside optically thick tissues. In particular, a morphological analysis of bladder urothelium using TPEF autofluorescence of NADH allowed the characterization of different urothelium state as such healthy mucosa (HM) and Carcinoma in situ (CIS) by means of nuclear-to-cytoplasm cellular ratio. Further characterization was obtained by means of spectral- and time-resolved detection of endogenous fluorescence. Combined spectral and lifetime analysis was able to discriminate tissue types of different morpho-functional characteristics. Compared to healthy bladder mucosa, CIS has shown differences in spectral emission (due to a different SHG contribution in the detected signal), as well as a different ratio of fast to slow NADH fluorescence lifetime. This multidimensional analysis may represent a powerful imaging tool, if combined with endoscopy or with cystoscopy, for the diagnosis of CIS and other bladder lesions.

2. MATERIALS AND METHODS

2.1 Multidimensional two-photon laser scanning microscope

The experimental setup (Fig. 1) is a custom-made upright microscope, developed in collaboration with the mechanical and electronic workshops of LENS, designed to perform two-photon laser scanning fluorescence microscopy (TPEF), conventional wide-field microscopy and fluorescence lifetime imaging microscopy (FLIM) with spectral resolved detection. All the microscope optics are fixed onto a custom vertical honeycomb steel breadboard 60 cm × 90 cm, 070BH0450 (Melles-Griot, Rochester, NY, US), mounted by two square brackets onto an anti-vibrating optical table 100 cm × 200 cm (TMC, Peabody, MA, US). For the white-light wide-field subsystem, the light source is a halogen lamp (HL) KL200 (Schott AG, Mainz, Germany) or a custom-made metallic ring with six superluminescent LEDs, to be used for trans- or epi-illumination of the sample, respectively. The image of the sample is collected by a color CCD camera COOLPIX 4700 (Nikon, Tokyo, Japan) using a tilting mirror (M5). For the two-photon excitation, a mode-locked Ti:Sapphire laser CHAMELEON (Coherent Inc, Santa Clara, CA, US), provides 120 fs pulses at a 90 MHz repetition rate, tunable in wavelength between 705 and 980 nm. The laser beam path includes a collimating telescope (L1, L2), a half wavelength broadband waveplate ($\lambda/2$) coupled with a calcite polarizing beam splitter (PBS) for laser power adjustment and a custom-made electronic shutter (S), before passing to the scanning head. The scanning head comprises two galvo mirrors (G1,G2) VM500 (GSI Lumonics, Munich, Germany), rotated about orthogonal pivots and coupled by a spherical mirrors pair (Sm1, Sm2). The laser beam is raster scanned by opportunely moving the two galvo mirrors, such that the beam focus is scanned in the focal plane of the objective lens with a pixel dwell time of typically 5 μs. A scanning lens (L3, f = 50 mm) and the microscope tube lens (TL, f = 200 mm) expand the beam to a dimension of around 1 cm, before it is focused onto the specimen by an objective XLUM 20×, N.A. 0.90, W.D. 2 mm (Olympus Co., Japan). A piezoelectric stage (PZT) PIFOC P-721 (Physik Instrumente GmbH, Karlsruhe, Germany) allows axial displacements of the objective up to 100 μm with sub-nanometer resolution, and hence the optical sectioning of the sample.

The detection system for the two photon fluorescence, is constituted by a dichroic filter (D1) 685DCXRU (Chroma Technology Corporation, Rockingham, VT, US) with 685 nm cut off wavelength. Fluorescence light is decoupled from the laser path in non-descanning mode. A two photon cut off filter (SBF) E700SP-2P (Chroma Technology Corporation, Rockingham, VT, US) eliminates laser light back reflections. Light passes through a lens (L4) and hits on a dichroic mirror (D2) FF456-Di01 (Semrock, Rochester, NY, US), before being focused onto the active area of two photomultiplier detectors (PMT) H7710-13 (Hamamatsu Photonics, Hamamatsu City, Japan), allowing simultaneous detection of two-photon fluorescence and second-harmonic generation. SHG is filtered by a narrow-band filter HQ420BP (Chroma Techology Corporation, Rockingham, VT, US). Detection can be switched to a second sub-system for time- and spectral-resolved measurements. A couple of lens (L4, L5), constituting a telescope, reduces the angle

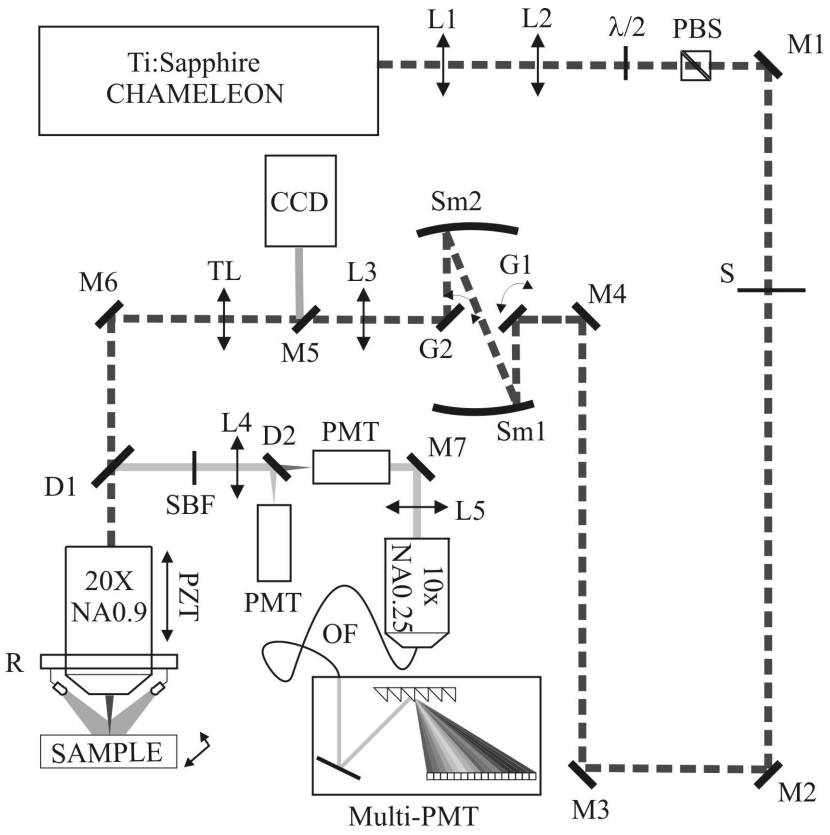

Figure 1. A schematic draw (b) of the multispectral two-photon experimental setup.

spanned by the fluorescence light during the scanning. An objective lens Plan 10×, 0.25 NA (Nikon, Tokyo, Japan) couples the fluorescence light in a multimode optical fiber (OF). The detector (Multi-PMT) PML-Spec (Becker & Hickl GmbH, Berlin, Germany) is constituted by a diffraction grating and a 16-channels multi-anode photomultiplier strip with 200 ps FWHM pulses. It allows spectral resolved (13 nm for each channel) measurements of fluorescence light with variable spectral range (overall range 200 nm). The detection has an upper wavelength limit of 685 nm set by the cut off optical filter, and a lower limit of 200 nm set by the detector response. During measurements, 420 nm – 620 nm range was used.

Acquisition and control are performed using a PC and two synchronized I/O boards, PCI-MIO-16E (National Instruments, Austin, TX, US) and SPC-730 (Becker & Hickl GmbH, Berlin, Germany). The two boards are synchronized by an electronic timing board E-6502 (National Instruments, Austin, TX, US). The output settings are controlled by a custom-made software developed in LabView ambient. The input settings and the visualization of the acquired images are accomplished using a dedicated software SPCM 1.1 (Becker & Hickl GmbH, Berlin, Germany) that also allows to change the photon counting board settings. Image pixels exponential fits, image de-convolution and analysis are performed using the software SPC-Image 2.8 (Becker&Hickl GmbH, Berlin, Germany).

3. RESULTS

3.1 Two-photon endogenous fluorescence of NADH

A morphological analysis can be accomplished from the acquired images. In particular, cells of healthy bladder mucosa (Figure 2a) appear more regular in distribution and shape with respect to the corresponding CIS cells (Figure 2b). Moreover, the nucleus (dark in the images) to cytoplasm (bright in the images) ratio of the represented cells is quite different between healthy bladder mucosa and CIS, as shown in the graph (Figure 2c) representing the averaged ratio

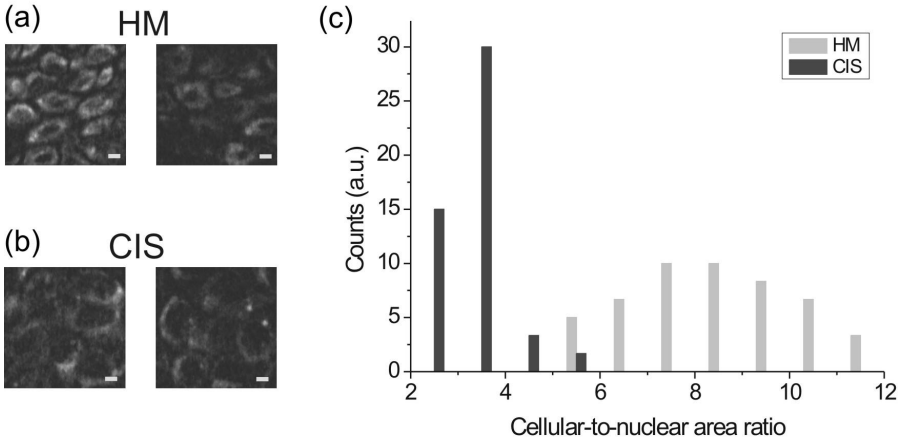

Figure 2. Two couple of representative images of healthy bladder mucosa (a) and Carcinoma in Situ (b) acquired at 30 μm depth from tissue surface on *ex-vivo* fresh biopsies. Images have been acquired using two-photon autofluorescence with 740 nm excitation wavelength. Scale bars: 3 μm. Histogram distribution of the cellular-to-nuclear area ratio (d) for CIS (in black) and for HM (in light gray), calculated by summing over 5 samples of CIS and 5 samples of HM and over 10 cells per samples.

over 5 samples of HM and CIS (10 cells per sample). The fluorescence intensity is higher in healthy samples with respect to the corresponding CIS sample, even if this datum is strongly affected by the biological variability and the time between excision and imaging.

3.2 Combined TPE-SHG for imaging tumor stroma

An additional morphological feature can highlighted by combined TPEF of NADH and SHG microscopy. In particular, the tumor stroma, represented by a network of collagen fibers flattened and mainly parallel to the tumor border can be imaged in 3-D, as shown (Figure 3), where a Z-stack of combined TPEF-SHG images is represented. The importance of such a capability in the early diagnosis and staging of bladder cancer resides in the relationship between the organization of collagen around the lesion and the invasiveness of the tumor. Up to now, it is still unclear how aggressive tumors act on collagen network in disrupting fibers to give rise to cellular penetration and proliferation in the connective tissue.

3.3 Fluorescence lifetime imaging of cellular NADH and FAD

A better analysis of the NADH and FAD fluorescence coming from urothelium can be performed by combining TPEF with fluorescence lifetime imaging microscopy (FLIM). We have acquired images of the urothelium in fresh biopsies of both HM and CIS, finding differences in the ratio between the two components. In this analysis we used a double-exponential decay function as a fitting function for fluorescence decay, in order to take into account both free- and protein-bound contributions. In fact, NADH and FAD fluorescence lifetime strongly depends on the fact that the molecules are in their free or protein-bound state. In general, when detecting NADH and FAD fluorescence, both contributions are present. In order to take into account both components, the decay function used for fitting fluorescence decay data was the following:

$$I_{Fluo} = a_1 \exp\left(\frac{-t}{\tau_1}\right) + a_2 \exp\left(\frac{-t}{\tau_2}\right);$$

where the free parameters are the following, provided the normalization $a_1+a_2=1$.

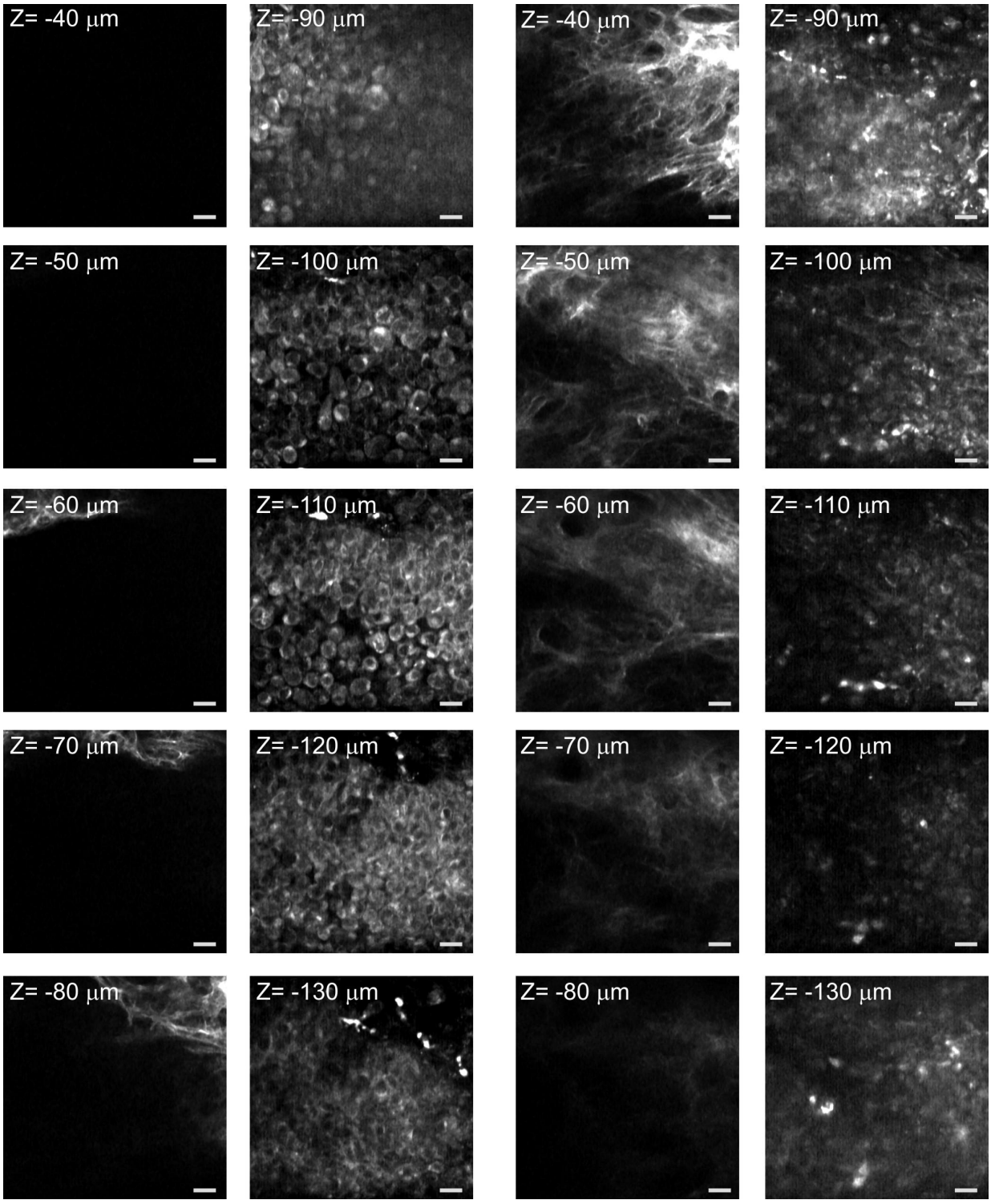

Figure 3. Two representative image Z-stacks (0.1 mm range) acquired with SHG microscopy (first and third column) and with TPEF microscopy (second and fourth column). TPEF and SHG were acquired using 740 nm and 840 nm excitation wavelength, respectively. Depths measured from tissue surface are indicated. Scale bars: 10 μm.

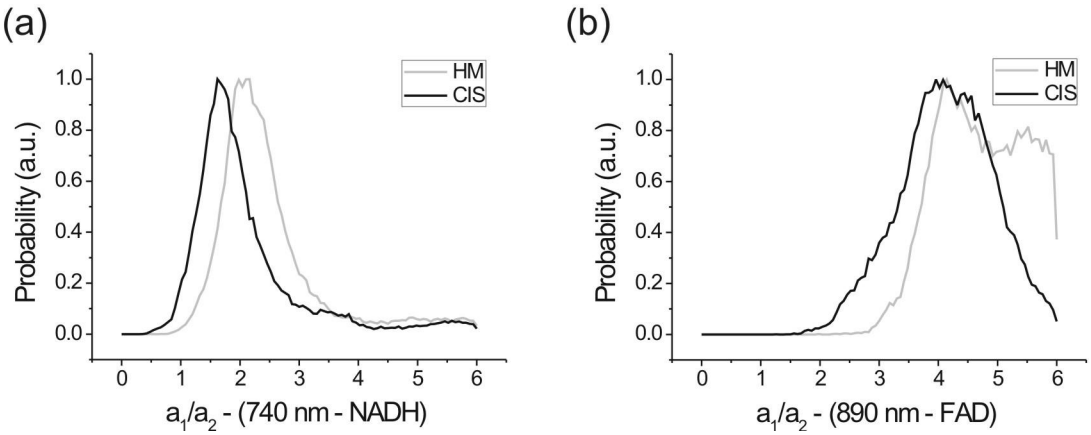

Figure 4. Lifetime components ratio distribution for CIS (black) and for HM (light grey), obtained by summing the calculated parameter over a cellular region of 128 μm × 128 μm, and after averaging on 5 samples of CIS and 5 samples of HM, using 740 nm (a), and 890 nm (b) as excitation wavelength.

$$\tau_1 : \text{fast lifetime component;}$$
$$\tau_2 : \text{slow lifetime component;}$$
$$\frac{a_1}{a_2} : \text{components ratio.}$$

Lifetime analysis was performed by using 740 nm and 890 nm excitation wavelength. Two fluorescence filters centered at 460 nm and 510 nm allowed to selectively detect NADH and FAD fluorescence, respectively. Fluorescence decay traces fits were performed after system response de-convolution by using a double-exponential decay function in order to take into account both free and protein-bound state of the two molecules. In the double-exponential decay model the fast component is related to free-NADH and the slow component to protein-bound NADH, and vice-versa for FAD. The three fit parameters are: the two lifetime components (fast and slow) and their coefficient ratio. In particular, the ratio of the components is representing the ratio free/protein-bound for NADH, and the ratio protein-bound/free for FAD. The two graphs in Fig. 3 are representing the distributions of the lifetime components ratio of both HM and CIS, calculated for excitation of NADH at 740 nm (Fig. 3a) and of FAD at 890 nm (Fig. 3b), averaged on 5 samples per tissue type. The obtained results showed that a higher relative concentration of protein-bound NADH and of free FAD is characterizing CIS in comparison to HM, where the opposite shift was found. An observation on tissue degradation should be done at this point, especially if considering degradation of samples and lifetime measurements. Even if in a tissue biopsy degradation, including oxidation, should start immediately after excision, NADH and FAD can be used to image a fresh tissue up to 4-5 hours after excision. Certainly, the time between excision and imaging can affect the measured values, especially for *ex-vivo* samples. Anyway, in a time-lapse measurement performed on two samples (data not shown), a negligible variation of fluorescence lifetime has been observed for both HM and CIS over 2 hours. The measurement started approximately one hour after excision. Even if some slightly different values are expected from *in-vivo* measurements, the method presented here can be considered a promising tool to optically record NADH/FAD Red-Ox state of a tissue and its application in *in-vivo* imaging could be useful in early diagnosis of cancerous and precancerous tissues, as well as in the follow-up of cancer-targeted therapies.

4. CONCLUSION

In conclusion, in this work we have demonstrated the capability of our multidimensional method to discriminate between healthy bladder mucosa and CIS on *ex-vivo* fresh biopsies of bladder tissue. We have found morphological and spectroscopic difference between the two tissue types. Even if further analysis, as well as a more significant statistics on a larger number of samples, is required to confirm our encouraging results, our method could become a promising tool to

be used in a multiphoton endoscope or in a spectroscopic probe with the final goal of improving white light cystoscopy diagnostic accuracy.

ACKNOWLEDGEMENT

We thank LENS (contract # TOK-MC-509761), Ente Cassa di Risparmio di Firenze, and FABLS (contract # ARC-2007) for their financial support to this project.

REFERENCES

[1] ACS (2006), http://www.cancer.org/downloads/STT/CAFF2006PWSecured.pdf, Cancer Facts & Figures (2006).

[2] Kah, J. C., Lau, W. K., Tan, P. H., Sheppard, C. J., and Olivo, M., "Endoscopic image analysis of photosensitizer fluorescence as a promising noninvasive approach for pathological grading of bladder cancer in situ," *J. Biomed. Opt.* 13(5), 054022 (2008).

[3] Larsen, E. L., Randeberg, L. L., Gederaas, O. A., Arum, C. J., Hjelde, A., Zhao, C. M., Chen, D., Krokan, H. E., and Svaasand, L. O., "Monitoring of hexyl 5-aminolevulinate-induced photodynamic therapy in rat bladder cancer by optical spectroscopy," *J. Biomed. Opt.* 13(4), 044031 (2008).

[4] Berrahmoune, S., Fotinos, N., Bezdetnaya, L., Lange, N., Guedenet, J. C., Guillemin F., and D'Hallewin, M. A., "Analysis of differential PDT effect in rat bladder tumor models according to concentration of hexyl-aminolevulinate," *Photochem. Photobiol. Sci.* 7(9), 1018-1024 (2008).

[5] Denk, W., Strickler, J. H., and Webb, W. W., "Two-photon laser scanning fluorescence microscope," *Science* 248, 73-76 (1990).

[6] Zipfel, W. R., Williams, R. M., and Webb, W. W., "Nonlinear magic: multiphoton microscopy in the biosciences," *Nat. Biotechnol.* 21, 1369-1377 (2003).

[7] Zoumi, A., Yeh, A., and Tromberg, B. J., "Imaging cells and extracellular matrix in vivo by using second harmonic generation and two-photon excited fluorescence, " *Proc. Natl. Acad. Sci. USA* 99, 11014-11019 (2002).

[8] Zipfel, W. R., Williams, R. M., Christie, R., Nikitin, A. Y., Hyman, B. T., and Webb, W.W., "Live tissue intrinsic emission microscopy using multiphoton-excited native fluorescence and second harmonic generation, " *Proc. Natl. Acad. Sci. USA* 100, 7075-7080 (2003).

[9] König, K. and Riemann, I., "High-resolution multiphoton tomography of human skin with subcellular spatial resolution and picosecond time resolution," *J. Biomed. Optic.* 8(3), 432-439 (2003).

[10] Moreaux, L, Sandre, O., Charpak, S., Blanchard-Desce, M., and Mertz, J., "Coherent scattering in multi-harmonic light microscopy," *Biophys. J.* 80(3), 1568-1574 (2001).

[11] Campagnola, P. J., and Loew, L. M., "Second-harmonic imaging microscopy for visualizing biomolecular arrays in cells, tissues and organisms," *Nat. Biotechnol.* 21, 1356-1360 (2003).

[12] Campagnola, P. J., Millard, A. C., Terasaki, M., Hoppe, P. E., Malone, C. J., and Mohler, W. A., "Three-dimensional high-resolution second-harmonic generation imaging of endogenous structural proteins in biological tissues," *Biophys. J.* 81, 493-508 (2002).

[13] Roth, S., and Freund, I., "Second harmonic generation in collagen," *J. Chem. Phys.* 70, 1637-1643 (1979).

[14] König, K., Schenke-Layland, K, Riemann, I., and Stock, U. A., "Multiphoton autofluorescence imaging of intratissue elastic fibers," *Biomaterials* 26, 495-500 (2005).

[15] Williams, R. M., Zipfel, W. R., and Webb, W. W., "Interpreting second-harmonic generation images of collagen I fibrils," *Biophys. J.* 88, 1377-1386 (2005).

[16] Tadrous, P.J., "Methods for imaging the structure and function of living tissues and cells: 2. Fluorescence lifetime imaging, " *J. Pathol.* 191, 229-234 (2000).

[17] Tadrous, P. J., Siegel, J., French, P. M. W., Shousha, S., Lalani, E. N., and Stamp, G. W. H., "Fluorescence lifetime imaging of unstained tissues: early results in human breast cancer," *J. Pathol.* 199, 309-317 (2003).

[18] Chen Y., and Periasamy, A., "Characterization of two-photon excitation fluorescence lifetime imaging microscopy for protein localization," *Microsc. Res. Tech.* 63(1), 72-80 (2004).

[19] Breusegem, S. Y., Levi, M., and Barry, N. P., "Fluorescence correlation spectroscopy and fluorescence lifetime imaging microscopy," *Nephron. Exp. Nephrol.* 103(2), e41-e49 (2006).

[20] Laiho, L. H., Pelet, S., Hancewicz, T. M., Kaplan, P. D., and So, P. T. C., "Two-photon 3-D mapping of ex vivo human skin endogenous fluorescence species based on fluorescence emission spectra," *J. Biomed. Opt.* 10(2), 024016 (2005).

[21] Cicchi, R., Massi, D., Sestini, S., Carli, P., De Giorgi, V., Lotti, T., and Pavone, F. S., "Multidimensional non-linear laser imaging of Basal Cell Carcinoma," *Opt. Express* 15, 10135-10148 (2007).